

1 **Duplicated zebrafish (*Danio rerio*) inositol phosphatases *inpp5ka* and *inpp5kb* diverged in expression pattern
2 and function**

3 Dhyanan Shukla^{1*}, Brian M. Gural^{1*}, Edmund S. Cauley^{2*}, Llion E. Roberts³, Brittany F. Karas¹, Luca Cavallo¹,
4 Luka Turkalj¹, Sally A. Moody⁴, Laura E. Swan³, M. Chiara Manzini¹

5 1. Department of Neuroscience and Cell Biology and Child Health Institute of New Jersey, Rutgers Robert Wood
6 Johnson Medical School, New Brunswick, NJ, USA

7 2. Department of Biochemistry and Molecular Medicine, School of Medicine and Health Sciences, The George
8 Washington University, Washington, DC, USA

9 3. Institute of Systems, Molecular and Integrative Biology, University of Liverpool, Liverpool, UK

10 4. Department of Anatomy and Cell Biology, School of Medicine and Health Sciences, The George Washington
11 University, Washington, DC, USA

12 * These authors contributed equally to the study

13 **Corresponding author:**

14 M. Chiara Manzini, PhD
15 89 French Street, CHINJ rm 3274
16 New Brunswick, NJ 08901
17 Email: chiara.manzini@rutgers.edu

18 **Abstract**

19 One hurdle in the development of zebrafish models of human disease is the presence of multiple zebrafish orthologs
20 resulting from whole genome duplication in teleosts. Mutations in Inositol polyphosphate 5-phosphatase K
21 (*INPP5K*) lead to a syndrome characterized by variable presentation of intellectual disability, brain abnormalities,
22 cataracts, muscle disease, and short stature. *INPP5K* is a phosphatase acting at position 5 of phosphoinositides to
23 control their homeostasis and is involved in insulin signaling, cytoskeletal regulation, and protein trafficking.
24 Previously, our group and others have replicated the human phenotypes in zebrafish knockdown models by targeting
25 both *INPP5K* orthologs *inpp5ka* and *inpp5kb*. Here, we show that *inpp5ka* is the more closely related orthologue to
26 human *INPP5K*. While both *inpp5ka* and *inpp5kb* mRNA expression levels follow a similar trend in the developing
27 head, eyes, and tail, *inpp5ka* is much more abundantly expressed in these tissues than *inpp5kb*. *In situ* hybridization
28 revealed a similar trend, also showing unique localization of *inpp5kb* in the pineal gland indicating different
29 transcriptional regulation. We also found that *inpp5kb* has lost its catalytic activity against its preferred substrate,
30 PtdIns(4,5)P₂. Since most human mutations are missense changes disrupting phosphatase activity, we propose that
31 loss of *inpp5ka* alone can be targeted to recapitulate the human presentation. In addition, we show that the function
32 of *inpp5kb* has diverged from *inpp5ka* and may play a novel role in the zebrafish.

33 **Keywords:** inositol phosphatase, INPP5K, zebrafish, gene duplication

40 **Introduction**

41 Inositol polyphosphate 5-phosphatase K (INPP5K [MIM:607875]) is a highly conserved phosphatase that
42 participates in the regulation of phosphoinositide (PI) signaling. Also referred to as skeletal muscle and kidney-
43 enriched inositol phosphatase (*SKIP*), *INPP5K* is highly expressed in the brain, eyes, and muscles during
44 development and adulthood (Gurung et al., 2003; Ijuin et al., 2000). In humans, homozygous or compound
45 heterozygous mutations in *INPP5K* have been causally linked to a form of congenital muscular dystrophy with
46 cataracts and intellectual disability (MIM: 617404) also associated with short stature, and microcephaly with
47 considerable variability in the age of onset and early presentations (D'Amico et al., 2020; Hathazi et al., 2021;
48 Osborn et al., 2017; Wiessner et al., 2017; Yousaf et al., 2017). Similarities have been noted with Marinesco-
49 Sjögren syndrome (MIM: 248800), a form of myopathy also associated with congenital cataracts, short stature, and
50 cerebellar ataxia (Krieger et al., 2013; Senderek et al., 2005).

51
52 PIs are a category of lipid molecules that play crucial roles in signal transduction, ion channel regulation,
53 cellular migration, membrane trafficking, vesicle transport, and many other processes (Balla, 2013; Paolo and
54 Camilli, 2006; Raghu et al., 2019). The seven unique members of this group are distinguished by their patterns of
55 phosphorylation of the phosphorylated inositol head (PtdIns), which can occur at one or more of three positions (-3,
56 -4, or -5). Production of PIs is regulated by an array of kinases and phosphatases (Balla, 2013). INPP5K hydrolyzes
57 the D-5 position of the inositol ring in both PtdIns(4,5)P₂ and PtdIns(3,4,5)P₃, with highest activity for PtdIns(4,5)P₂
58 (Davies et al., 2015; Ijuin et al., 2000; Vandeput et al., 2006). INPP5K is largely localized to the endoplasmic
59 reticulum (ER) (Dong et al., 2018; Gurung et al., 2003) but can translocate to membrane ruffles as part of a complex
60 with the glucose regulated protein GRP78/BiP to negatively regulate insulin receptor signaling via
61 phosphatidylinositol-3-kinase (PI3K) (Ijuin and Takenawa, 2003; Ijuin et al., 2015, 2016a, 2016b).

62
63 Multiple zebrafish (*Danio rerio*) models of *INPP5K* loss of function have been generated using morpholino
64 oligonucleotides (MOs) targeting both paralogs, *inpp5ka* and *inpp5kb* (Hathazi et al., 2021; Osborn et al., 2017;
65 Wiessner et al., 2017). However, when the genes were targeted independently, knockdown of *inpp5ka* was sufficient
66 to yield phenotypes typical of neurological and muscular disorders, such as microphthalmia, microcephaly,
67 shortened body, reduced touch-evoked motility and myopathy. In contrast, *inpp5kb* MOs produced a mild phenotype
68 in a small subset of morphants (Osborn et al., 2017). In addition, we found *inpp5ka* expression to be 16-fold higher
69 than *inpp5kb* in zebrafish embryos at 2 days post fertilization (dpf) (Osborn et al., 2017). These findings suggested
70 that *inpp5ka* may be the most conserved human paralog and *inpp5kb* function may have diverged.

71
72 Due to a genome duplication event in teleost fish, about 30% of zebrafish genes have a paralog (Howe et al.,
73 2013), but duplicated genes often acquire differential expression and function (Postlethwait et al., 1998; Ravi and
74 Venkatesh, 2018). In this study we sought to better characterize expression patterns and function of *inpp5ka* and
75 *inpp5kb* to understand whether they diverged and support the development of better models of *INPP5K* mutations in
76 humans. We show that both *inpp5ka* and *inpp5kb* have a dynamic developmental expression in the eyes, head, and
77 tail, also finding that despite being expressed at lower levels, *inpp5kb* is specifically enriched in the pineal gland.
78 Inpp5kb lost the majority of its phosphatase activity for PtdIns(4,5)P₂ which is the preferred substrate for INPP5K
79 (Ijuin et al., 2000). Together, these data indicate that *inpp5ka* is the closest ortholog to *INPP5K* and suggest a unique
80 role for *inpp5kb* within the zebrafish.

81 **Methods**

82 *Animal Care*

83 Maintenance and husbandry of zebrafish (*Danio rerio*) breeders and larvae were performed following protocols
84 approved by the Institutional Animal Care and Use Committee of the George Washington University and Rutgers
85 University. All animals were from the AB background.

86 *Protein alignments*

87 QIAGEN CLC Sequence Viewer 8 was used to align the sequences for all transcripts. Percent identities between the
88 human INPP5K (NP_057616.2), zebrafish Inpp5ka (NP_001082962.2), and Inpp5kb (XP_021335020.1) were
89 calculated using EMBOSS Needle (Madeira et al., 2022).

90 *Quantitative PCR (qPCR) analysis*

91 Samples were collected at 1, 2, 3, 4 and 5 dpf. Whole zebrafish embryos and larvae or micro-dissected tissue from
92 eyes, head, and tails were pooled and RNA was extracted using the ReliaPrep RNA Miniprep System kit (Promega,

96 Madison, WI). RNA was treated with DNase I (New England Biolabs, Ipswich, MA) and complementary DNA
97 (cDNA) was synthesized using the iScript cDNA Synthesis kit (Bio-Rad, Hercules, CA). 600 ng of cDNA per
98 sample were analyzed via qPCR using the SsoFast EvaGreen Supermix (Bio-Rad, Hercules, CA) on a Bio-Rad
99 CFX384 Touch Real Time PCR System. All reactions were run with 3 technical replicates and repeated on at least 3
100 biological replicates. Sequences for custom primers for *inpp5ka* and *inpp5kb* and housekeeping controls elongation
101 factor 1 alpha *eef1a* and riboprotein L13 *rpl13* are available upon request.
102

103 *Whole-mount in situ hybridization (ISH)*

104 Full length *inpp5ka* (NM_001089493.1) and *inpp5kb* (XM_021479345.1) cDNAs were cloned into the pCS2+
105 plasmid (Addgene, Watertown, MA). Digoxigenin-labeled sense and antisense probes were synthesized from the
106 linearized plasmids using the DIG RNA Labeling Kit (SP6/T7) (Roche/MilliporeSigma, Burlington, MA). Whole-
107 mount ISH was performed as previously described (Yan et al., 2009).

108 *Phosphatase assay*

109 Full length *inpp5ka* (NM_001089493.1) and *inpp5kb* (XM_021479345.1) cDNAs were generated by gene synthesis
110 and cloned into the pGEX-1 to generate GST-fusion proteins (Genewiz/Azenta Life Sciences, South Plainfield, NJ).
111 GST-human INPP5K and GST were used as positive and negative controls respectively (Weissner et al., 2017).
112 Constructs were transformed into BL21 DE3 pLysS, induced with 100uM IPTG overnight and harvested by
113 centrifugation. Cells were lysed in assay buffer (50 mM Tris-HCl [pH 7.5], 150 mM NaCl, 10 mM MgCl₂) plus 1%
114 Triton X-100, EDTA-free protease inhibitors (Roche Diagnostics) and turbonuclease (Sigma). GST fusion proteins
115 were affinity purified over Gluthione Sepharose 4B (GE Healthcare). After extensive washing, aliquots of beads
116 were run on Coomassie gels to determine the abundance of full-length fusion proteins. Beads bearing equal amounts
117 of fusion proteins were incubated in assay buffer containing 135 μ M PtdIns(4,5)P₂diC8 or PtdIns(3,4,5)P₃diC8,
118 including control wells with no enzyme or no substrate lipid, and incubated for 1h at 37C. Free phosphate was
119 measured using the Malachite Green assay kit (Echelon Biosciences). Results of three independent experiments
120 were presented as mean \pm standard deviation. To minimize variability between purifications, all constructs were
121 freshly prepared and purified in parallel for each experiment.
122

123

124

Results

125

Zebrafish and human INPP5K protein alignments

126

To determine whether *inpp5ka* and *inpp5kb* lead to functionally divergent proteins, we first analyzed their protein sequence. Protein sequence alignment of INPP5K (NP_057616.2), Inpp5ka (NP_001082962.2), and Inpp5kb (XP_021335020.1) (Fig. 1) revealed 42.6% and 38.5% identity between the human orthologue and Inpp5ka and Inpp5kb respectively, while the zebrafish proteins showed 56% identity with each other. Inpp5kb has an additional 48 amino acid N-terminal sequence that was not present in either Inpp5ka or INPP5K.

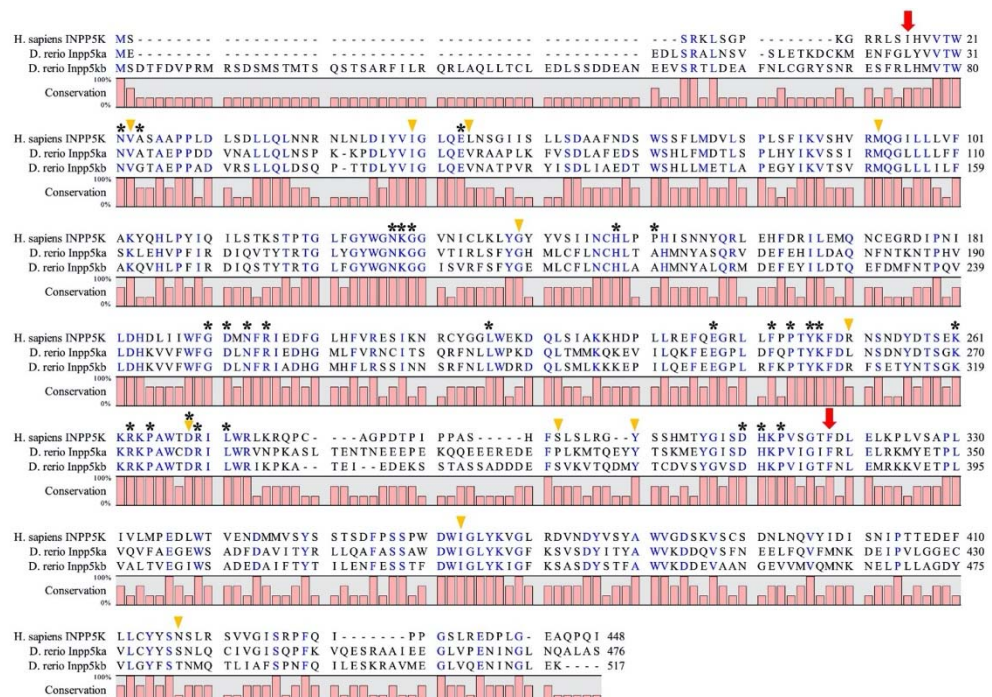


Figure 1. Protein alignment of INPP5K, Inpp5ka and Inpp5kb highlighting conserved amino acids required for phosphatase activity. The start and end of the catalytic domain in the human protein are marked with arrows. Amino acids required for phosphatase activity have been denoted with asterisks (*). Arrowheads indicate residues that are altered by missense variants in humans.

131

132

133

134

135

Divergent expression and localization of INPP5K orthologs in zebrafish larva

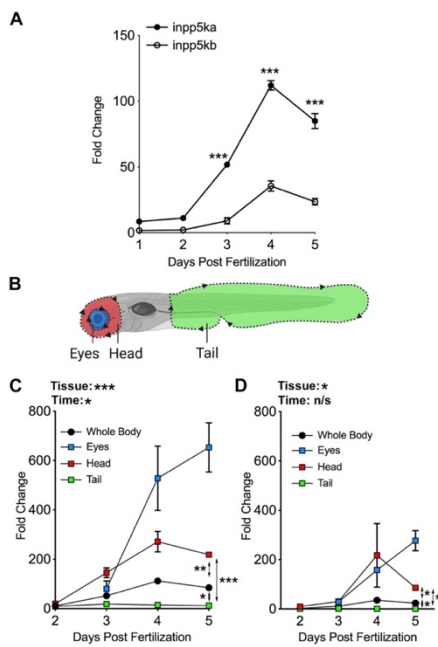
136

137

138 Analysis of *inpp5ka* and *inpp5kb* mRNA obtained from whole zebrafish embryos had shown higher expression of *inpp5ka* (Osborn et al., 2017). We used qPCR to define expression patterns throughout the first five days of development. We found that *inpp5ka* (NM_001089493.1) was consistently expressed much more abundantly than *inpp5kb* (XM_021479345.1) (Fig. 2A). The developmental expression trend was similar for *inpp5ka* and *inpp5kb*. Both genes had relatively low levels of expression at 1- and 2-dpf, but gene expression peaked at 4 dpf, where we saw a 3.2-fold difference between the two paralogs. Gene expression started decreasing in the following day (Fig. 2A, Fold change relative to 1dpf *inpp5kb*. *inpp5ka*: 2dpf 11.1±1.5, 3dpf 51.9±0.4, 4dpf 112.1±3.6, 5dpf 84.9±5.7; *inpp5kb*: 2dpf 2.1±0.1, 3dpf 9.0±2.3, 4dpf 35.5±3.9, 5dpf 23.6±2.5. p>0.0001 at 3, 4, and 5 dpf).

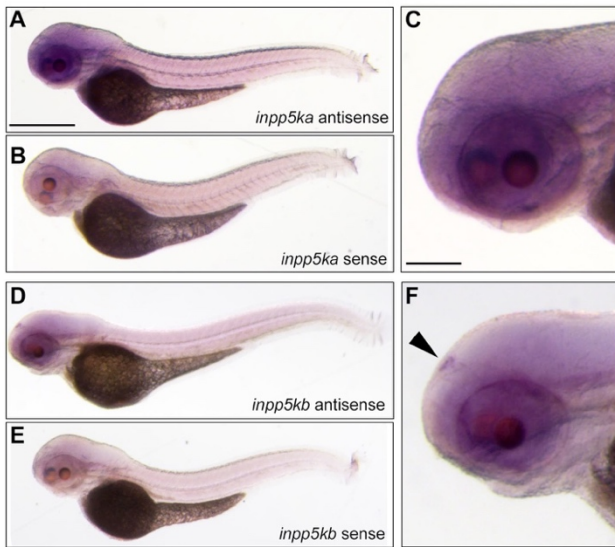
146

147 Loss of *INPP5K* in humans affects the muscle, brain, and eyes and knockdown of *inpp5ka* in zebrafish larvae 148 resulted in morphological abnormalities in the eyes and skeletal muscle (Hathazi et al., 2021; Osborn et al., 2017; 149 Wiessner et al., 2017). We dissected the heads, eyes, and tails of developing larvae for tissue-specific expression 150 analysis (Fig. 2B). This revealed that, while *inpp5ka* was consistently expressed at higher levels, both paralogs 151 exhibit the greatest expression in the eyes and head. *inpp5ka* and *inpp5kb* showed 4.7- and 4.4-fold higher 152 expression in the eyes respectively when compared to the whole-body at 4 dpf. The head revealed a 2.4-fold 153 difference in *inpp5ka* and a 6.1-fold difference in *inpp5kb* compared to the whole-body expression (Fig. 2C-D, Fold 154 change relative to 1dpf *inpp5kb*. *inpp5ka*: 3dpf head 145.2±19.3, eyes 80.4±31.6; 4dpf head 271.2±41.5, eyes 155 528.1±129.8; 5dpf 218.5±2.7, eyes 653.1±99.6. *inpp5kb*: 3dpf head 30.4±3.4, eyes 28.6±4.4; 4dpf head 156 217.3±128.8, eyes 157.7±8.4; 5dpf head 85.8±7.9, eyes 276.9±40.6).



157
158 **Figure 2. *inpp5ka* and *inpp5kb* mRNAs differ in expression in zebrafish larvae.** A. Gene expression determined
159 by qPCR. *inpp5ka* is more highly expressed in whole body lysates through 5 dpf. B. Larval tissues were excised
160 from the eye, head, and tail for localized gene expression analysis. C-D. Expression for both *inpp5ka* (C) and
161 *inpp5kb* (D) is low in the tail and increases in the eyes and brain. By 5 dpf, both are most highly expressed in the
162 eyes. Values are averages \pm SEM. * p < 0.05, ** p < 0.01, *** p < 0.001
163

164 To determine whether the expression patterns were consistent, we conducted *in-situ* hybridization on whole-
165 mount larvae at 3 dpf. *inpp5ka* antisense probing reflected the results of our previous gene expression assays.
166 *inpp5ka* mRNA was most abundant in the head and eyes, with lower expression in the tail (Fig. 3A-C). As expected,
167 *inpp5kb* antisense targeting revealed moderate expression throughout the head and eyes (Fig. 3D-E). However, in
168 contrast with *inpp5ka*, *inpp5kb* was abundantly expressed in the pineal gland (Fig. 3F), a neuroendocrine organ
169 which responds to light and plays a role in circadian rhythm (Cahill, 1996; Livne et al., 2016; Vatine et al., 2011).
170 These findings indicate that in addition to lower expression, *inpp5kb* also diverged in its expression pattern.



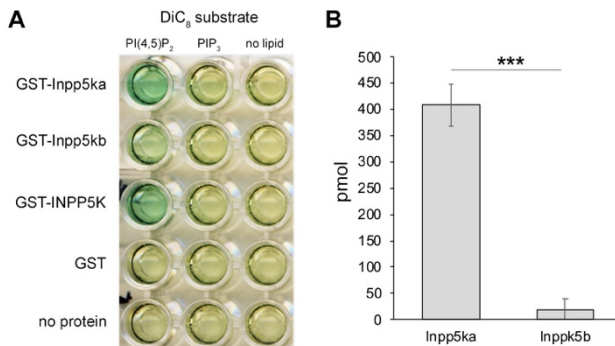
171
172 **Figure 3. *inpp5ka* and *inpp5kb* mRNAs differ in localization in zebrafish larvae.** A-C. *In situ* hybridization in 3
173 dpf larvae shows that *inpp5ka* mRNA is highly expressed throughout the head and eyes. Scale bars: 500 μ m in A,

174 100μm in C. **D-F.** *inpp5kb* expression is concentrated to the pineal gland. The pineal gland is indicated by the black
175 arrow.

176

177 *Divergence in phosphatase activity of human and zebrafish orthologs of INPP5K*

178 To evaluate the preservation of the PI phosphatase activity in the zebrafish isoforms, we conducted a malachite
179 phosphatase assay to examine the activity of INPP5K and the two zebrafish Inpp5k isoforms against the preferred
180 substrate PtdIns(4,5)P₂ (**Fig. 4A**). We found that zebrafish Inpp5ka and human INPP5K were both highly active
181 against PtdIns(4,5)P₂. This activity was specific, as illustrated by the lack of phosphatase activity against PIP₃.
182 However, compared to Inpp5ka, Inpp5kb was nearly inactive against PtdIns(4,5)P₂. Inpp5ka yielded 409 pmol of
183 free phosphate vs 20pmol for Inpp5kb, indicating that Inpp5ka had a 20-fold higher activity compared to Inpp5kb
184 (**Fig. 4B**).



185
186 **Figure 4. Inpp5ka and Inpp5kb exhibit different phosphatase activity.** **A.** Phosphatase activity of human
187 INPP5K, Inpp5ka and Inpp5kb in malachite assay. Human INPP5K and Inpp5ka demonstrate high activity for the
188 PI(4,5)P₂ substrate. PIP₃ did not elicit activity from any isoform. **B.** Inpp5ka is more significantly active against
189 diC8PI(4,5)P₂ compared to Inpp5kb. Values are averages ± SEM. *** p < 0.001 following t-test.
190

191 The INPP5K protein is primarily composed of a 5-phosphatase domain between amino acids 16-318 and a
192 SKITCH domain between amino acids 321-448. Most found mutations in humans are missense and have been
193 shown to reduce or ablate phosphatase activity (Osborn et al., 2017; Wiessner et al., 2017). We wondered whether
194 the loss in activity in Inpp5kb could be caused by changes in amino acids identified to be critical for the catalytic
195 activity of INPP5K. Basing this analysis on the available crystal structures of other Type II inositol phosphate 5-
196 phosphatases, *INPP5B* and *SYNJI* (Paesmans et al., 2020; Trésaugues et al., 2014), we found that all sites were
197 conserved in Inpp5ka and Inpp5kb and there were no major changes that could explain differences in activity
198 (asterisks in **Fig. 1**). We also assessed whether residues known to be affected by pathogenic variants in patients were
199 conserved in Inpp5kb, and these amino acids were all maintained (arrowheads in **Fig. 1**) (D'Amico et al., 2020;
200 Osborn et al., 2017; Hathazi et al., 2021; Wiessner et al., 2017; Yousaf et al., 2017). Thus, possible changes on
201 known residues do not explain the difference in function between Inpp5ka and Inpp5kb.
202

203 **Discussion**

204 *INPP5K* mutations in humans cause a distinct neurodevelopmental syndrome with variable presentation of
205 intellectual disability, cataracts, short stature, and muscle disease (D'Amico et al., 2020; Osborn et al., 2017;
206 Wiessner et al., 2017; Yousaf et al., 2017). Multiple zebrafish models have been developed to study *inpp5k* function
207 using morpholino oligonucleotides either blocking translation or knocking down mRNA expression (Hathazi et al.,
208 2021; Osborn et al., 2017; Wiessner et al., 2017). However, the presence of duplicated *inpp5k* genes, *inpp5ka* and
209 *inpp5kb*, in zebrafish complicates the development of both candidate loss- and gain-of-function mutations since both
210 zebrafish orthologs may need to be targeted. Initial functional data from our previous studies had shown that
211 *inpp5ka* knockdown alone was sufficient to replicate the findings in the double gene knockdown (Osborn et al.,
212 2017). In this study, we show that *inpp5ka* and *inpp5kb* have diverged in expression levels, patterns and function
213 following teleost whole genome duplication (WGD). *inpp5ka*, rather than *inpp5kb*, maintains a higher sequence
214 identity to human *INPP5K*, suggesting that genetic removal of this gene may be sufficient to recapitulate the human
215 mutation.

216 Polyploidization by WGD is a significant driver of evolution (Postlethwait et al., 1998; Sémon and Wolfe,
217 2007). During the period of re-diploidization that follows a WGD event, most redundant genes are eliminated via

218 genomic rearrangements and mutations causing one duplicated copy to become a pseudogene. However, a
219 duplicated gene may be preserved and gradually diverge in expression patterns and/or function during evolution
220 leading to gene adaptation through sub-functionalization or neo-functionalization of one of the duplicated genes
221 (Kassahn et al., 2009; Sémon and Wolfe, 2007). While *inpp5ka* is broadly and highly expressed throughout the
222 zebrafish larvae, *inpp5kb* is significantly less expressed. Additionally, we found that Inpp5kb exhibits minimal
223 phosphatase activity against the traditional substrate of INPP5K, PtdIns(4,5)P₂ (Ijuin et al., 2000; Vandeput et al.,
224 2006). While both paralogs are most abundant in the head, the visualization of expression achieved by *in-situ*
225 hybridization reveals that the expression of *inpp5kb* is specifically enriched in the pineal gland. The pineal gland is
226 thought to be the master regulator for circadian rhythm in vertebrates. Melatonin is the key circadian hormone
227 secreted by the pineal gland in zebrafish (Cahill, 1996) and is thought to play a role in locomotor activity (Livne et
228 al., 2016), as well in the timing of reproduction and feeding (Piccinetti et al., 2013). It will be interesting in the
229 future to determine whether Inpp5kb is involved in pineal functions independently of its phosphatase activity.

230 In humans, much of the pathology resulting from mutations within *INPP5K* have been attributed to the
231 dysregulation of phosphoinositide homeostasis (Hathazi et al., 2021; McGrath et al., 2020; Osborn et al., 2017;
232 Wiessner et al., 2017). Most known mutations in *INPP5K* are missense variants occurring in the catalytic
233 phosphatase domain reducing or ablating conversion of PtdIns(4,5)P₂ to PtdIns(4)P (Osborn et al., 2017; Wiessner et
234 al., 2017). In the muscle, *INPP5K* is involved in insulin signaling through the PI3K/Akt/mTOR pathway (Ijuin and
235 Takenawa, 2015; Ijuin et al., 2015), but recent studies in a muscle-specific *Inpp5k* mouse knock-out line also
236 determined that abnormal accumulation of PtdIns(4,5)P₂ led to a severe disruption in lysosome recycling (McGrath
237 et al., 2020). Interestingly, lysosome enlargement and autophagy inhibition found in the *Inpp5k*-deficient muscle
238 were not dependent of Akt/mTOR signaling, suggesting an independent additional role for PtdIns(4,5)P₂ in muscle
239 maintenance in the autophagic lysosome reformation pathway (McGrath et al., 2020). In addition, increased levels
240 of D3-phosphoglycerate dehydrogenase (PHGDH) have been found in fibroblasts obtained from individuals with
241 *INPP5K* phosphatase mutations, indicating further metabolic disruptions (Hathazi et al., 2021). Overall, we propose
242 that targeting the phosphatase domain in Inpp5ka would lead to a reliable model for *INPP5K* mutations in humans.
243

244 Whether Inpp5kb evolved to perform a different function in the pineal gland and how it lost its phosphatase
245 activity in the zebrafish remains to be studied.
246

247 **Acknowledgements**

248 The authors would like to thank all members of the Manzini laboratory for helpful discussion, Kathleen Flaherty and
249 Heather Pond for management of the zebrafish colonies at Rutgers University and the George Washington
250 University, respectively, and Himani Majumdar for assistance with the *in situ* protocols.
251 This work was funded by the National Institutes of Health R01NS109149 to M.C.M, Wellcome Trust
252 (105616/Z/14/Z) and the Medical Research Council (MRC/N010035/1) to L.E.S. Additional support was provided
253 to M.C.M. from the Robert Wood Johnson Foundation (grant #74260).
254

255 **Author contributions**

256 M.C.M. and E.S.C. conceived the study. D.S., B.M.G., E.S.C., L.E.R., B.F.K., L.C. and L.T. performed experiments
257 and collected data. D.S., B.M.G., E.S.C. and L.T. analyzed the data. D.S., B.M.G. and M.C.M. wrote the manuscript
258 with contributions from S.A.M. and L.E.S. All authors reviewed the manuscript.
259

260 **Competing Interests**

261 The authors declare no competing interests

262 **References**

263

264 Balla, T. (2013). Phosphoinositides: Tiny Lipids With Giant Impact on Cell Regulation. *Physiol Rev* 93, 1019–
265 1137. <https://doi.org/10.1152/physrev.00028.2012>.

266 Cahill, G.M. (1996). Circadian regulation of melatonin production in cultured zebrafish pineal and retina. *Brain Res*
267 708, 177–181. [https://doi.org/10.1016/0006-8993\(95\)01365-2](https://doi.org/10.1016/0006-8993(95)01365-2).

268 D'Amico, A., Fattori, F., Nicita, F., Barresi, S., Tasca, G., Verardo, M., Pizzi, S., Moroni, I., Mitri, F.D., Frongia, A., et al. (2020). A Recurrent Pathogenic Variant of INPP5K Underlies Autosomal Recessive Congenital Muscular Dystrophy With Cataracts and Intellectual Disability: Evidence for a Founder Effect in Southern Italy. *Frontiers Genetics* 11, 565868. <https://doi.org/10.3389/fgene.2020.565868>.

272 Davies, E.M., Kong, A.M., Tan, A., Gurung, R., Sriratana, A., Bukczynska, P.E., Ooms, L.M., McLean, C.A., Tiganis, T., and Mitchell, C.A. (2015). Differential SKIP expression in PTEN-deficient glioblastoma regulates cellular proliferation and migration. *Oncogene* 34, 3711–3727. <https://doi.org/10.1038/onc.2014.303>.

275 Dong, R., Zhu, T., Benedetti, L., Gowrishankar, S., Deng, H., Cai, Y., Wang, X., Shen, K., and Camilli, P.D. (2018). The inositol 5-phosphatase INPP5K participates in the fine control of ER organization. *The Journal of Cell Biology* 217, 3577–3592. <https://doi.org/10.1083/jcb.201802125>.

278 Gurung, R., Tan, A., Ooms, L.M., McGrath, M.J., Huysmans, R.D., Munday, A.D., Prescott, M., Whisstock, J.C., and Mitchell, C.A. (2003). Identification of a novel domain in two mammalian inositol-polyphosphate 5-phosphatases that mediates membrane ruffle localization. The inositol 5-phosphatase skip localizes to the endoplasmic reticulum and translocates to membrane ruffles following epidermal growth factor stimulation. *The Journal of Biological Chemistry* 278, 11376–11385. <https://doi.org/10.1074/jbc.m209991200>.

283 Hathazi, D., Cox, D., D'Amico, A., Tasca, G., Charlton, R., Carlier, R.-Y., Baumann, J., Kollipara, L., Zahedi, R.P., Feldmann, I., et al. (2021). INPP5K and SIL1 associated pathologies with overlapping clinical phenotypes converge through dysregulation of PHGDH. *Brain awab133-*. <https://doi.org/10.1093/brain/awab133>.

286 Howe, K., Clark, M.D., Torroja, C.F., Torrance, J., Berthelot, C., Muffato, M., Collins, J.E., Humphray, S., McLaren, K., Matthews, L., et al. (2013). The zebrafish reference genome sequence and its relationship to the human genome. *Nature* 496, 498–503. <https://doi.org/10.1038/nature12111>.

289 Ijuin, T., and Takenawa, T. (2003). SKIP negatively regulates insulin-induced GLUT4 translocation and membrane ruffle formation. *Molecular and Cellular Biology* 23, 1209–1220. <https://doi.org/10.1128/mcb.23.4.1209-1220.2003>.

291 Ijuin, T., and Takenawa, T. (2015). Improvement of insulin signaling in myoblast cells by an addition of SKIP-binding peptide within Pak1 kinase domain. *Biochemical and Biophysical Research Communications* 456, 41–46. <https://doi.org/10.1016/j.bbrc.2014.11.031>.

294 Ijuin, T., Mochizuki, Y., Fukami, K., Funaki, M., Asano, T., and Takenawa, T. (2000). Identification and characterization of a novel inositol polyphosphate 5-phosphatase. *The Journal of Biological Chemistry* 275, 10870–10875. .

297 Ijuin, T., Hatano, N., Hosooka, T., and Takenawa, T. (2015). Regulation of insulin signaling in skeletal muscle by PIP3 phosphatase, SKIP, and endoplasmic reticulum molecular chaperone glucose-regulated protein 78. *Biochimica et Biophysica Acta* 1853, 3192–3201. <https://doi.org/10.1016/j.bbamcr.2015.09.009>.

300 Ijuin, T., Hatano, N., and Takenawa, T. (2016a). Glucose-regulated protein 78 (GRP78) binds directly to PIP3 phosphatase SKIP and determines its localization. *Genes to Cells* □: Devoted to Molecular & Cellular Mechanisms 21, 457–465. <https://doi.org/10.1111/gtc.12353>.

303 Ijuin, T., Hosooka, T., and Takenawa, T. (2016b). Phosphatidylinositol 3,4,5-Trisphosphate Phosphatase SKIP Links Endoplasmic Reticulum Stress in Skeletal Muscle to Insulin Resistance. *Molecular and Cellular Biology* 36, 108–118. <https://doi.org/10.1128/mcb.00921-15>.

306 Kassahn, K.S., Dang, V.T., Wilkins, S.J., Perkins, A.C., and Ragan, M.A. (2009). Evolution of gene function and regulatory control after whole-genome duplication: Comparative analyses in vertebrates. *Genome Res* 19, 1404–1418. <https://doi.org/10.1101/gr.086827.108>.

309 Krieger, M., Roos, A., Stendel, C., Claeys, K.G., Sonmez, F.M., Baudis, M., Bauer, P., Bornemann, A., Goede, C.
310 de, Dufke, A., et al. (2013). SIL1 mutations and clinical spectrum in patients with Marinesco-Sjögren syndrome.
311 *Brain* \square : A Journal of Neurology 136, 3634–3644. <https://doi.org/10.1093/brain/awt283>.

312 Livne, Z.B.-M., Alon, S., Vallone, D., Bayleyen, Y., Tovin, A., Shainer, I., Nisembaum, L.G., Aviram, I., Smadja-
313 Storz, S., Fuentes, M., et al. (2016). Genetically Blocking the Zebrafish Pineal Clock Affects Circadian Behavior.
314 *Plos Genet* 12, e1006445. <https://doi.org/10.1371/journal.pgen.1006445>.

315 McGrath, M.J., Eramo, M.J., Gurung, R., Sriratana, A., Gehrig, S.M., Lynch, G.S., Lourdes, S.R., Koentgen, F.,
316 Feeney, S.J., Lazarou, M., et al. (2020). Defective lysosome reformation during autophagy causes skeletal muscle
317 disease. *J Clin Invest* 131. <https://doi.org/10.1172/jci135124>.

318 Osborn, D.P.S., Pond, H.L., Mazaheri, N., Dejardin, J., Munn, C.J., Mushref, K., Cauley, E.S., Moroni, I., Pasanisi,
319 M.B., Sellars, E.A., et al. (2017). Mutations in INPP5K Cause a Form of Congenital Muscular Dystrophy
320 Overlapping Marinesco-Sjögren Syndrome and Dystroglycanopathy. *American Journal of Human Genetics* 100,
321 537–545. <https://doi.org/10.1016/j.ajhg.2017.01.019>.

322 Paesmans, J., Martin, E., Deckers, B., Berghmans, M., Sethi, R., Loeys, Y., Pardon, E., Steyaert, J., Verstreken, P.,
323 Galicia, C., et al. (2020). A structure of substrate-bound Synaptosomal1 provides new insights in its mechanism and
324 the effect of disease mutations. *Elife* 9, e64922. <https://doi.org/10.7554/elife.64922>.

325 Paolo, G.D., and Camilli, P.D. (2006). Phosphoinositides in cell regulation and membrane dynamics. *Nature* 443,
326 651–657. <https://doi.org/10.1038/nature05185>.

327 Piccinetti, C.C., Migliarini, B., Olivotto, I., Simoniello, M.P., Giorgini, E., and Carnevali, O. (2013). Melatonin and
328 Peripheral Circuitries: Insights on Appetite and Metabolism in *Danio Rerio*. *Zebrafish* 10, 275–282.
329 <https://doi.org/10.1089/zeb.2012.0844>.

330 Postlethwait, J.H., Yan, Y.-L., Gates, M.A., Horne, S., Amores, A., Brownlie, A., Donovan, A., Egan, E.S., Force,
331 A., Gong, Z., et al. (1998). Vertebrate genome evolution and the zebrafish gene map. *Nat Genet* 18, 345–349.
332 <https://doi.org/10.1038/ng0498-345>.

333 Raghu, P., Joseph, A., Krishnan, H., Singh, P., and Saha, S. (2019). Phosphoinositides: Regulators of Nervous
334 System Function in Health and Disease. *Front Mol Neurosci* 12, 208. <https://doi.org/10.3389/fnmol.2019.00208>.

335 Ravi, V., and Venkatesh, B. (2018). The Divergent Genomes of Teleosts. *Annu Rev Anim Biosci* 6, 47–68.
336 <https://doi.org/10.1146/annurev-animal-030117-014821>.

337 Sémon, M., and Wolfe, K.H. (2007). Consequences of genome duplication. *Curr Opin Genet Dev* 17, 505–512.
338 <https://doi.org/10.1016/j.gde.2007.09.007>.

339 Senderek, J., Krieger, M., Stendel, C., Bergmann, C., Moser, M., Breitbach-Faller, N., Rudnik-Schöneborn, S.,
340 Blaschek, A., Wolf, N.I., Harting, I., et al. (2005). Mutations in SIL1 cause Marinesco-Sjögren syndrome, a
341 cerebellar ataxia with cataract and myopathy. *Nature Genetics* 37, 1312–1314. <https://doi.org/10.1038/ng1678>.

342 Trésaugues, L., Silvander, C., Flodin, S., Welin, M., Nyman, T., Gräslund, S., Hammarström, M., Berglund, H., and
343 Nordlund, P. (2014). Structural Basis for Phosphoinositide Substrate Recognition, Catalysis, and Membrane
344 Interactions in Human Inositol Polyphosphate 5-Phosphatases. *Structure* 22, 744–755.
345 <https://doi.org/10.1016/j.str.2014.01.013>.

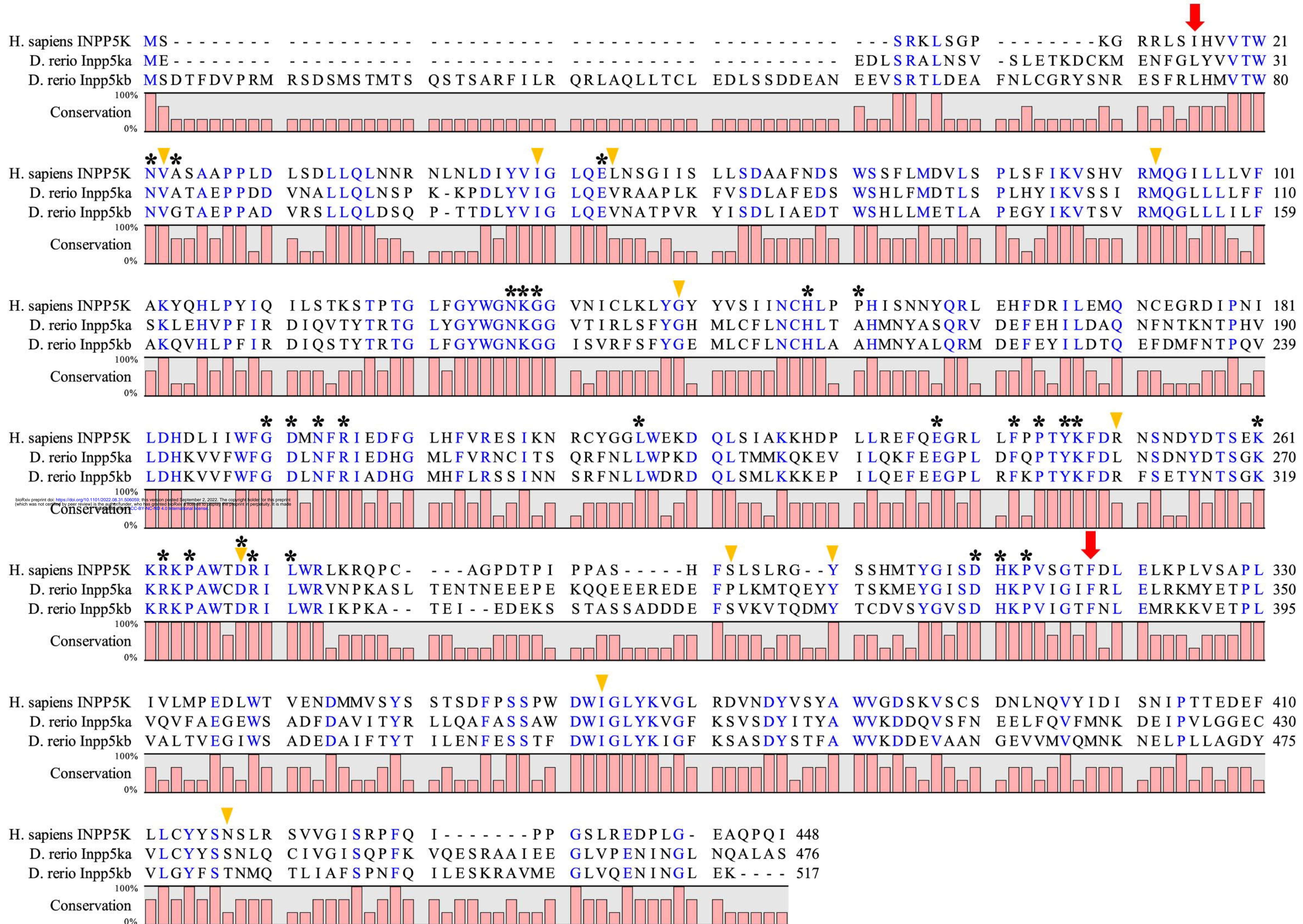
346 Vandeput, F., Backers, K., Villeret, V., Pesesse, X., and Erneux, C. (2006). The influence of anionic lipids on SHIP2
347 phosphatidylinositol 3,4,5-trisphosphate 5-phosphatase activity. *Cell Signal* 18, 2193–2199.
348 <https://doi.org/10.1016/j.cellsig.2006.05.010>.

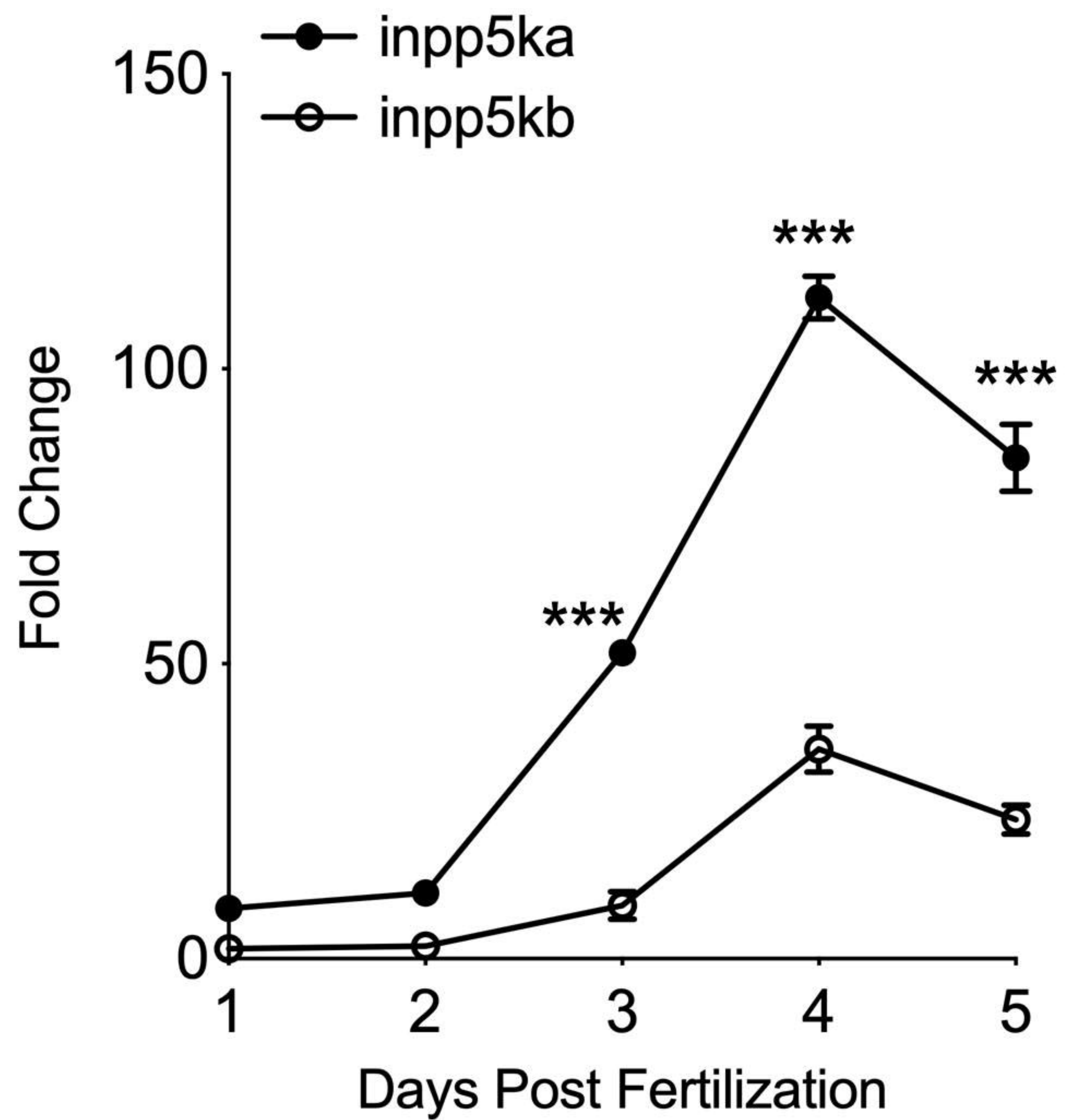
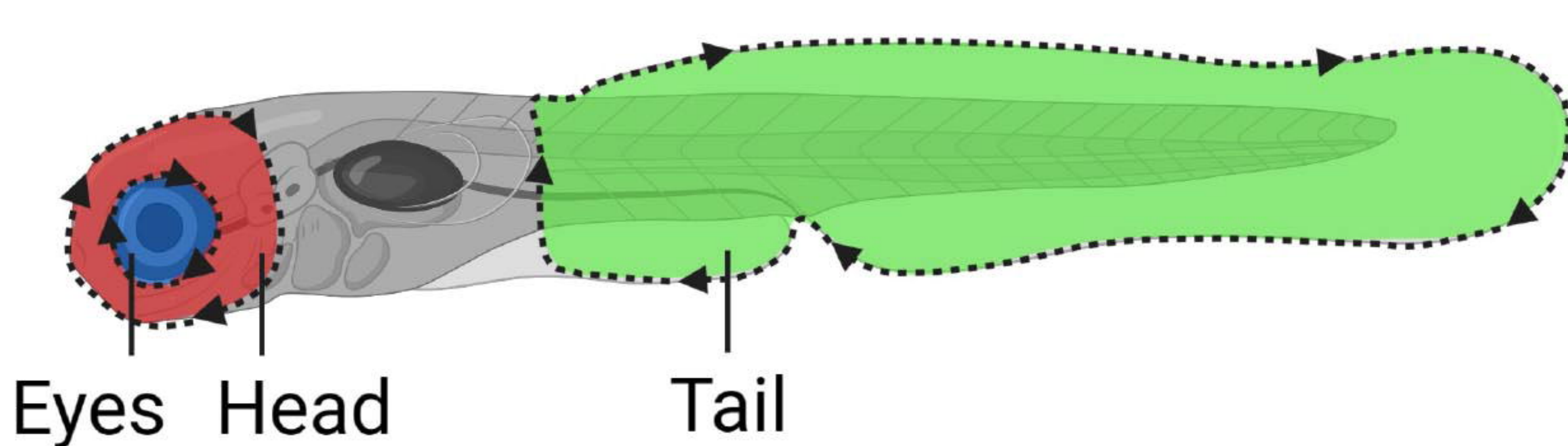
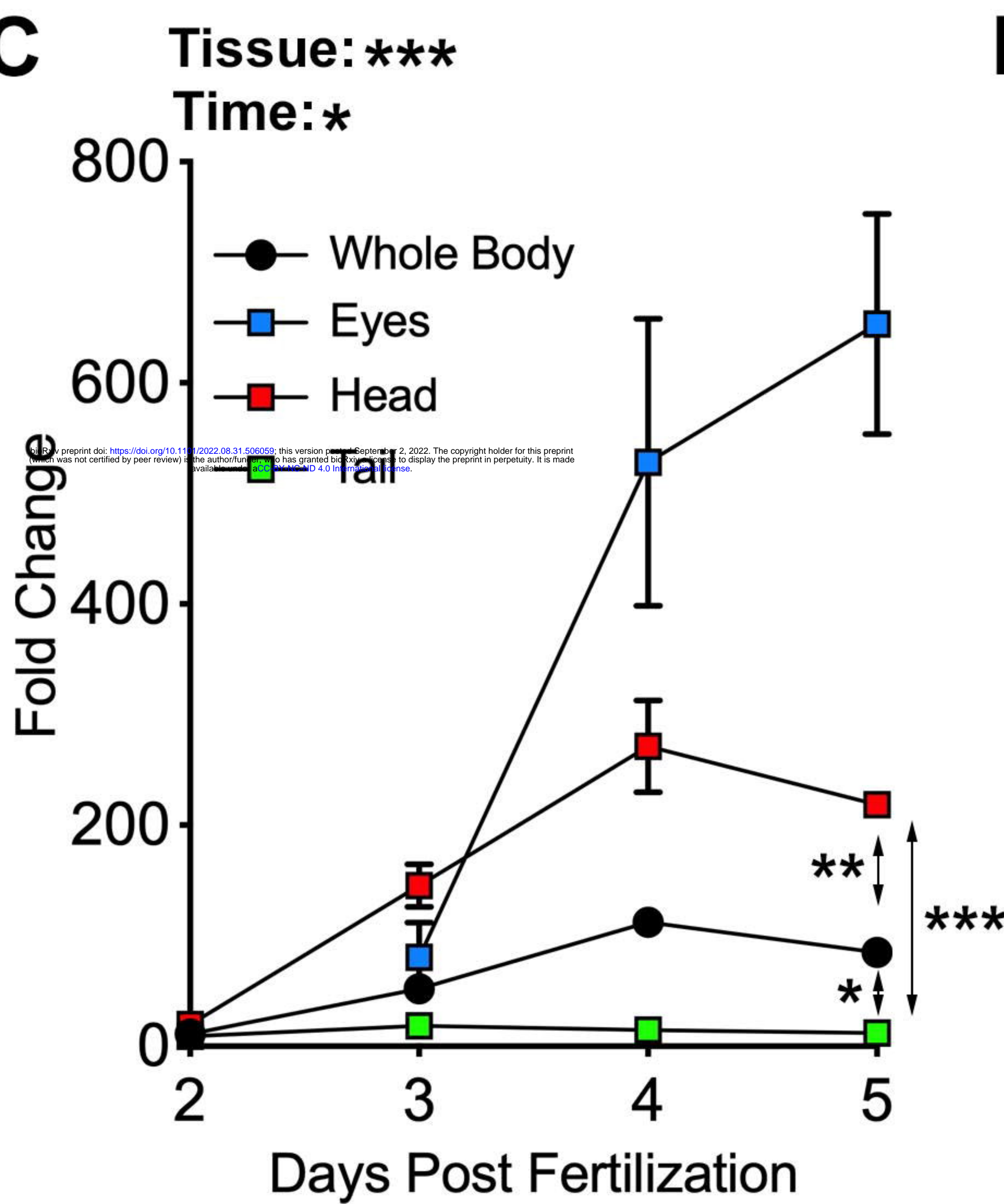
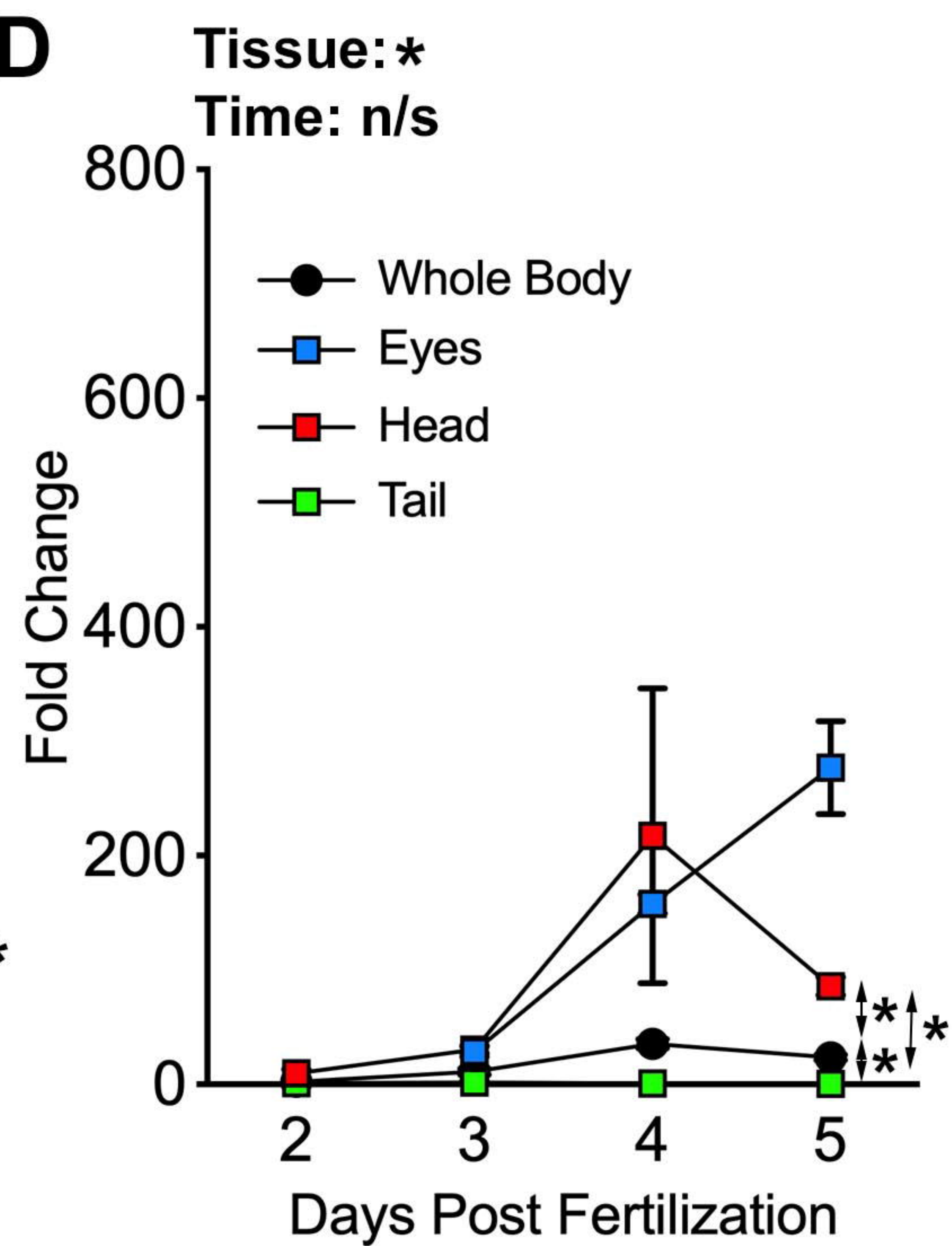
349 Vatine, G., Vallone, D., Gothilf, Y., and Foulkes, N.S. (2011). It's time to swim! Zebrafish and the circadian clock.
350 *Febs Lett* 585, 1485–1494. <https://doi.org/10.1016/j.febslet.2011.04.007>.

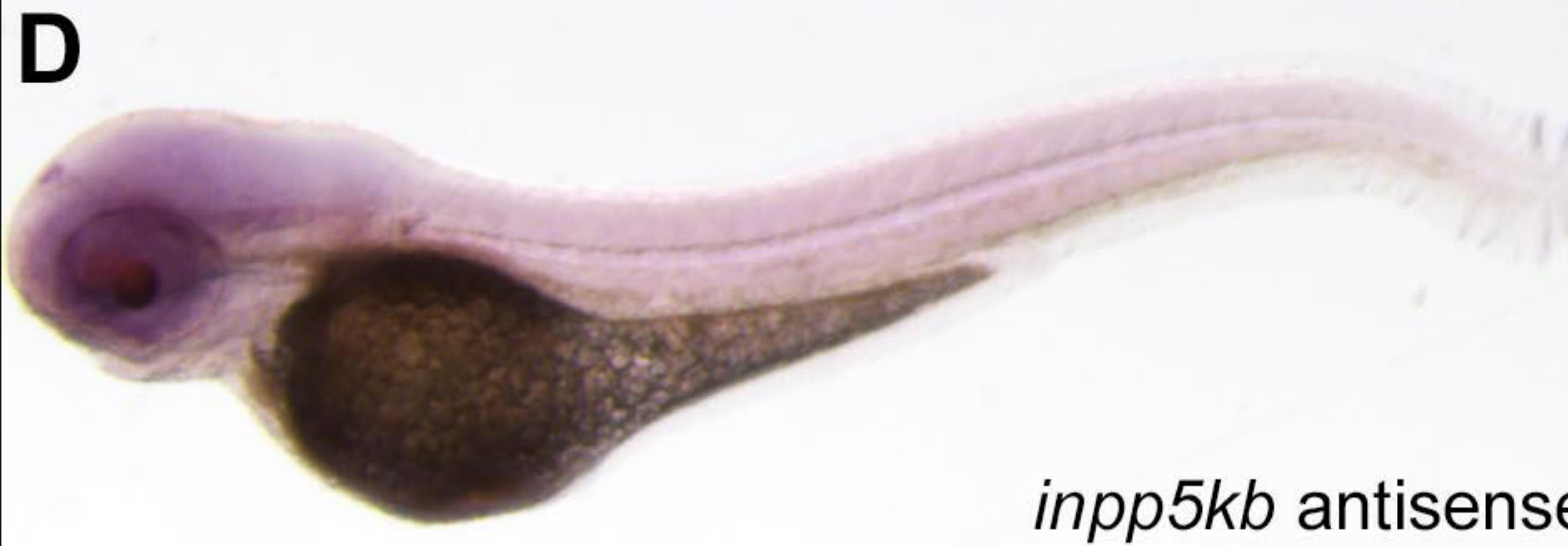
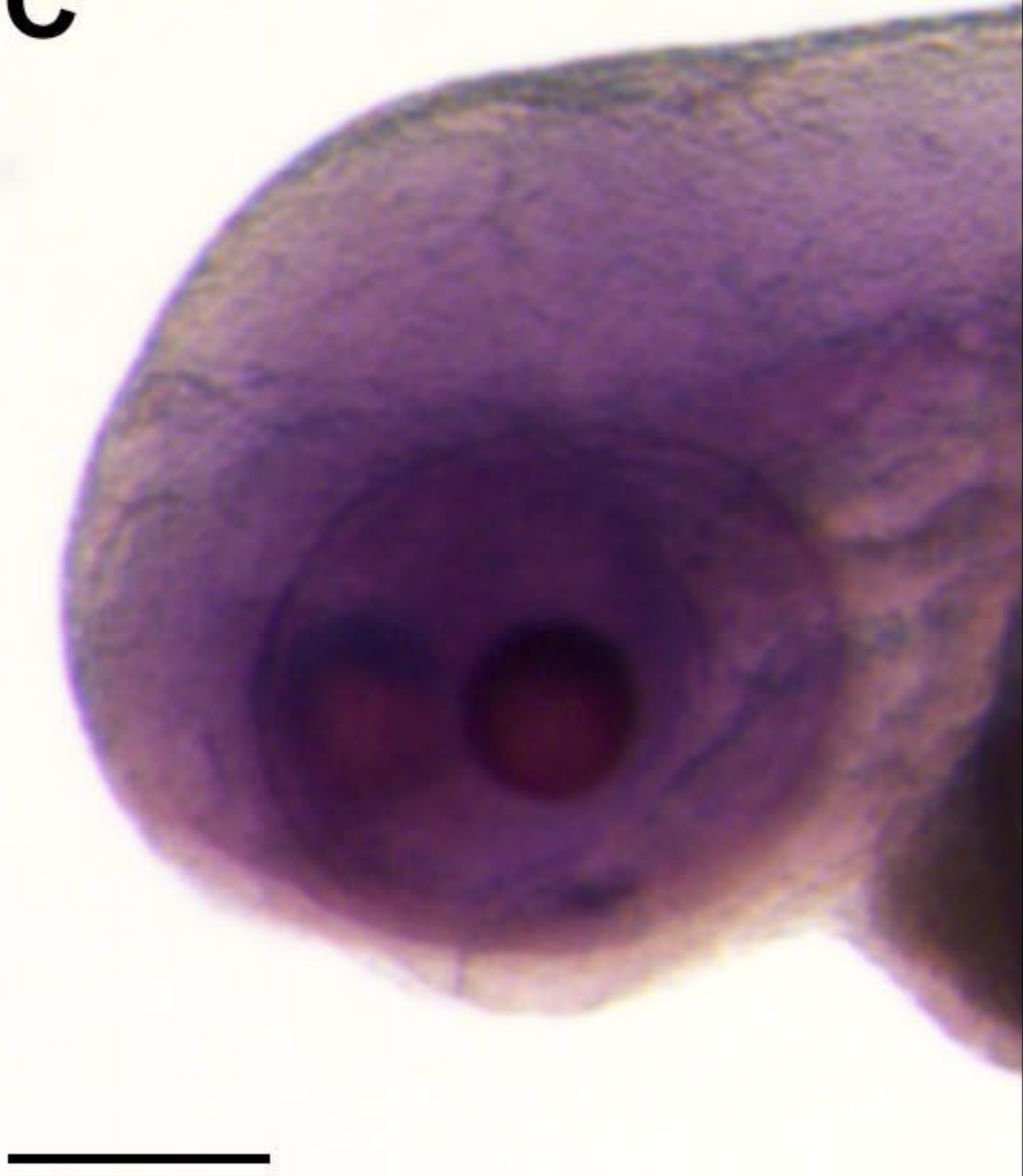
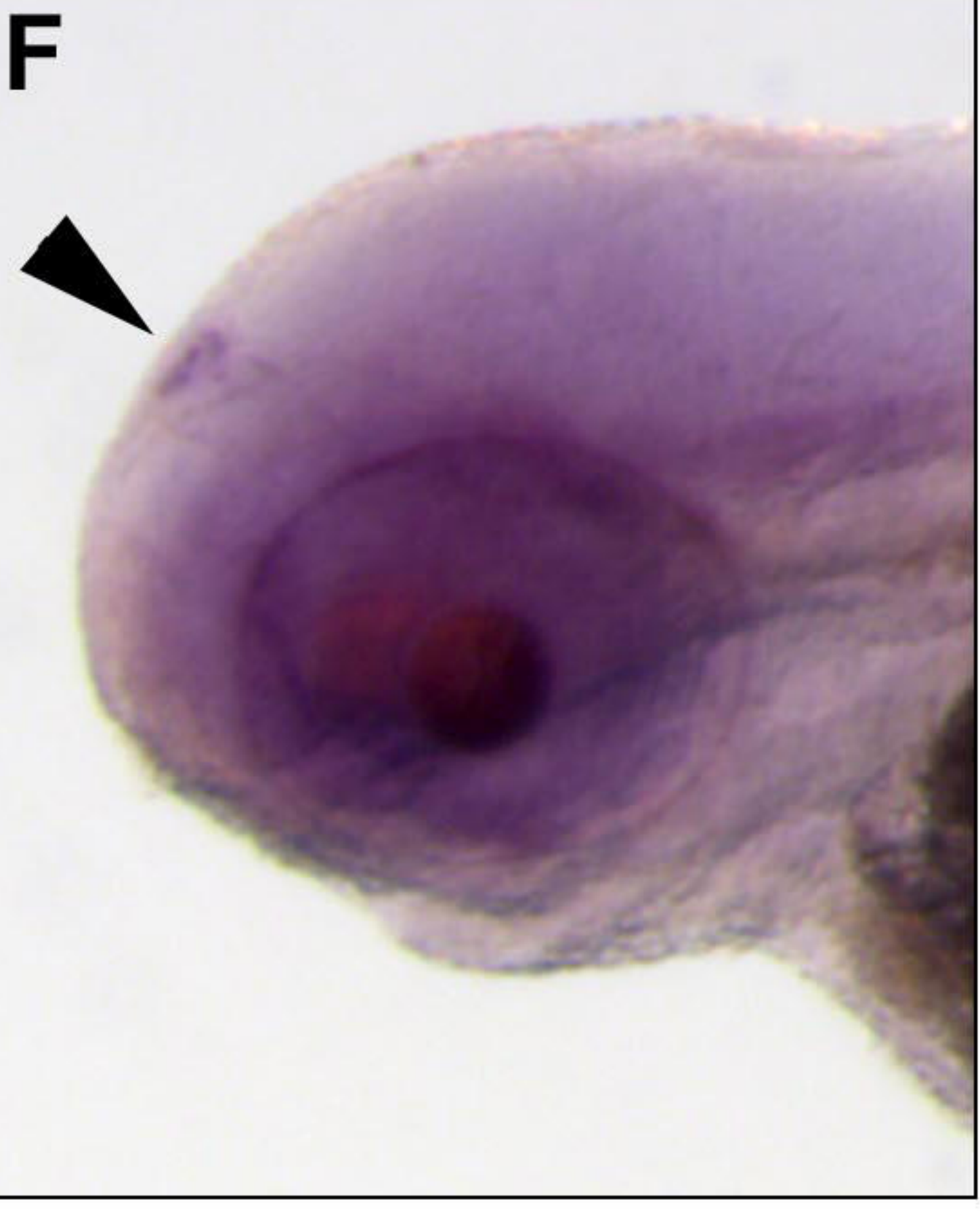
351 Wiessner, M., Roos, A., Munn, C.J., Viswanathan, R., Whyte, T., Cox, D., Schoser, B., Sewry, C., Roper, H.,
352 Phadke, R., et al. (2017). Mutations in INPP5K, Encoding a Phosphoinositide 5-Phosphatase, Cause Congenital
353 Muscular Dystrophy with Cataracts and Mild Cognitive Impairment. *American Journal of Human Genetics* 100,
354 523–536. <https://doi.org/10.1016/j.ajhg.2017.01.024>.

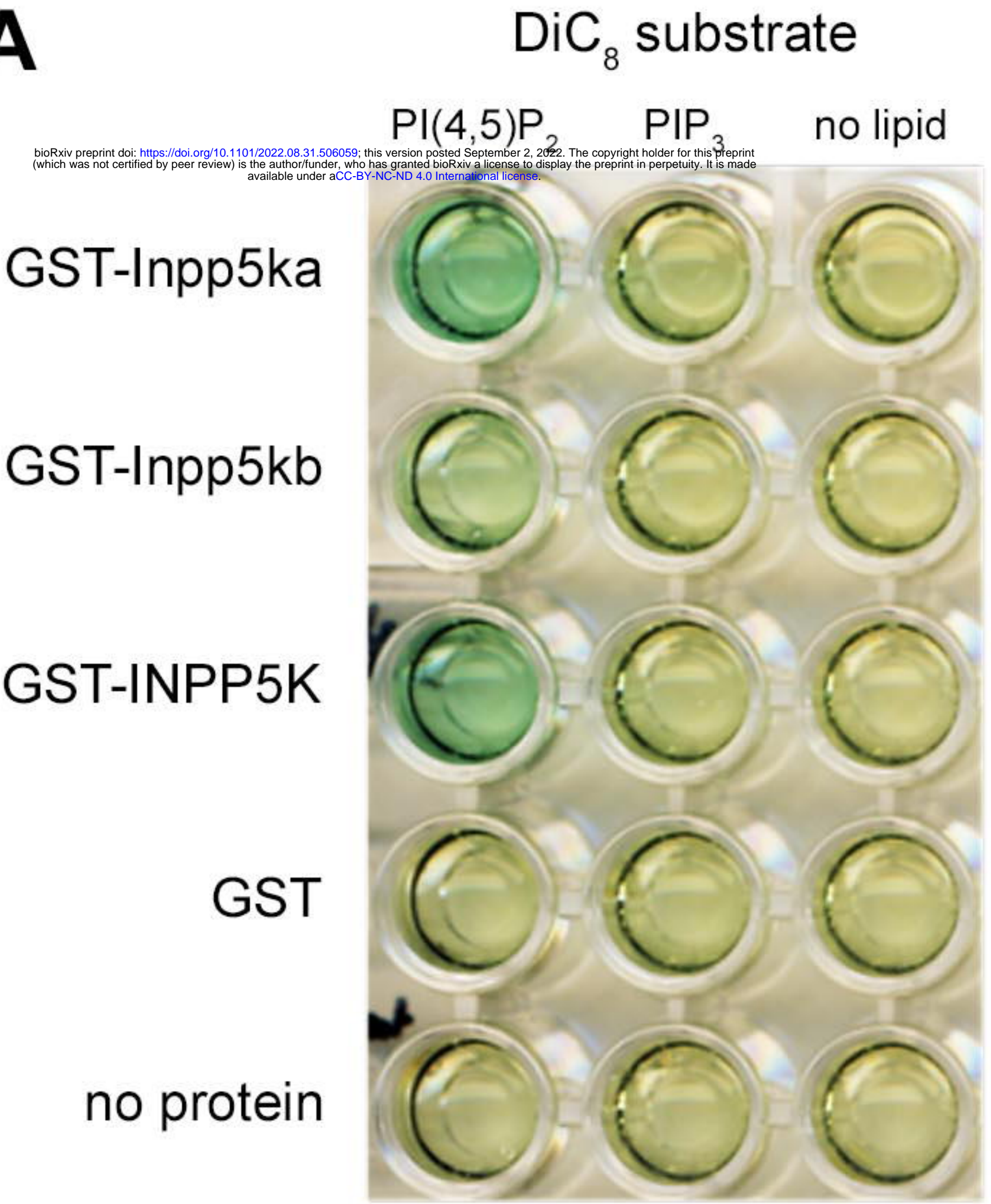
355 Yan, B., Neilson, K.M., and Moody, S.A. (2009). foxD5 plays a critical upstream role in regulating neural
356 ectodermal fate and the onset of neural differentiation. *Dev Biol* 329, 80–95.
357 <https://doi.org/10.1016/j.ydbio.2009.02.019>.

358 Yousaf, S., Sheikh, S.A., Riazuddin, S., Waryah, A.M., and Ahmed, Z.M. (2017). INPP5K variant causes autosomal
359 recessive congenital cataract in a Pakistani family. *Clinical Genetics* <https://doi.org/10.1111/cge.13143>.



A**B****C****D**

A**B****D****E****C****F**

A**B**